

Features of W production in p-p, p-Pb and Pb-Pb collisions

François Arleo

Laboratoire Leprince-Ringuet, École polytechnique, CNRS/IN2P3 91128 Palaiseau, France.

E-mail: francois.arleo@cern.ch

Émilien Chapon

CERN, Experimental Physics Department, CERN, CH-1211 Geneva 23, Switzerland,

Laboratoire Leprince-Ringuet, École polytechnique, CNRS/IN2P3 91128 Palaiseau, France.

E-mail: emilien.chapon@cern.ch

Hannu Paukkunen*

University of Jyväskylä, Department of Physics, P.O. Box 35, FI-40014 University of Jyväskylä, Finland

Helsinki Institute of Physics, P.O. Box 64, FI-00014 University of Helsinki, Finland

Instituto Galego de Física de Altas Enerxías (IGFAE), Universidade de Santiago de Compostela, E-15782 Galicia, Spain.

E-mail: hannu.paukkunen@jyu.fi

We consider the production of inclusive W bosons in variety of high-energy hadronic collisions: p-p, p- \bar{p} , p-Pb, and Pb-Pb. In particular, we focus on the resulting distributions of charged leptons from W decay that can be measured with relatively low backgrounds. The leading-order expressions within the collinearly factorized QCD indicate that the center-of-mass energy dependence at forward/backward rapidities should be well approximated by a simple power law. The scaling exponent is related to the small- x behaviour of the quark distributions, which is largely driven by the parton evolution. An interesting consequence is the simple scaling law for the lepton charge asymmetry which relates measurements in different collision systems. The expectations are contrasted with the existing data and a very good overall agreement is found. Finally, we propose precision observables to be measured at the LHC.

XXV International Workshop on Deep-Inelastic Scattering and Related Subjects

3-7 April 2017

University of Birmingham, UK

*Speaker.

1. Theoretical background

In this talk, we summarize the main findings of our recent article [1] in which we consider the inclusive production of W^\pm bosons in the leptonic decay channel,

$$H_1 + H_2 \rightarrow W^- + X \rightarrow \ell^- + \bar{\nu} + X,$$

$$H_1 + H_2 \rightarrow W^+ + X \rightarrow \ell^+ + \nu + X.$$

In particular, for a reason explained later, we will focus on the region with large leptonic rapidity $|y| \gg 0$. To understand what we are after, it is enough to examine the leading-order expressions for these processes in an approximation where the width Γ_W of W is much less than its mass M_W . At particular center-of-mass (c.m.) energy \sqrt{s} , the cross sections differential in lepton rapidity y and transverse momentum p_T read (see Ref. [1] for details),

$$\begin{aligned} \frac{d^2\sigma^{\ell^\pm}(s)}{dydp_T} &\approx \frac{\pi^2}{24s} \left(\frac{\alpha_{\text{em}}}{\sin^2\theta_W} \right)^2 \frac{1}{M_W\Gamma_W} \frac{p_T}{\sqrt{1-4p_T^2/M_W^2}} \sum_{i,j} |V_{ij}|^2 \delta_{e_{q_i}+e_{\bar{q}_j},\pm 1} \\ &\left\{ \left[1 \mp \sqrt{1-4p_T^2/M_W^2} \right]^2 q_i^{H_1}(x_1^+) \bar{q}_j^{H_2}(x_2^+) + \left[1 \pm \sqrt{1-4p_T^2/M_W^2} \right]^2 q_i^{H_1}(x_1^-) \bar{q}_j^{H_2}(x_2^-) + \right. \\ &\left. \left[1 \pm \sqrt{1-4p_T^2/M_W^2} \right]^2 \bar{q}_j^{H_1}(x_1^+) q_i^{H_2}(x_2^+) + \left[1 \mp \sqrt{1-4p_T^2/M_W^2} \right]^2 \bar{q}_j^{H_1}(x_1^-) q_i^{H_2}(x_2^-) \right\}, \end{aligned} \quad (1.1)$$

where the momentum arguments of the PDFs $q_i^{H_1}$ and $q_i^{H_2}$ are

$$x_1^\pm \equiv \frac{M_W^2 e^y}{2p_T \sqrt{s}} \left[1 \mp \sqrt{1-4p_T^2/M_W^2} \right], \quad x_2^\pm \equiv \frac{M_W^2 e^{-y}}{2p_T \sqrt{s}} \left[1 \pm \sqrt{1-4p_T^2/M_W^2} \right]. \quad (1.2)$$

Symbols α_{em} , θ_W and V_{ij} denote the QED coupling, weak-mixing angle, and CKM matrix. The electric charges of the quarks are marked by e_{q_i} . Defining a scaling variable $\xi_1 \equiv \frac{M_W}{\sqrt{s}} e^y$, we see that the momentum fractions x_1^\pm can be written as

$$x_1^\pm \rightarrow \frac{M_W}{2p_T} \xi_1 \left[1 \mp \sqrt{1-4p_T^2/M_W^2} \right]. \quad (1.3)$$

This implies that the cross-sections at fixed ξ_1 are sensitive to the PDFs of hadron H_1 at particular values of x , independently of \sqrt{s} . The qualitative difference between considering cross sections at fixed rapidity or fixed ξ_1 is illustrated in Figure 1: If the rapidity y is kept constant, the cross sections with two different c.m. energies \sqrt{s} and $\sqrt{s'}$, probe the PDFs at different ranges of x (left panel). However, if the scaling variable ξ_1 is maintained fixed instead, one samples the larger- x PDFs (assuming $y > 0$) at the same values of x (right panel) irrespective of the c.m. energy.

By making some further simplifications, we are able to derive rather simple scaling laws. Approximating the small- x PDFs at large interaction scale Q^2 by a power law

$$x\bar{q}_i(x, Q^2) \approx xq_i(x, Q^2) \approx N_i x^{-\beta(Q^2)}, \quad x \ll 1, \quad (1.4)$$

where $\beta \equiv \beta(Q^2 = M_W^2) \approx 0.35$ [1], it follows that

$$\frac{d\sigma^{\ell^\pm}(\sqrt{s}, \xi_1)}{d\xi_1} \approx (\sqrt{s})^{2\beta} \times F^\pm(\xi_1, H_1, H_2), \quad y \gg 0, \quad (1.5)$$

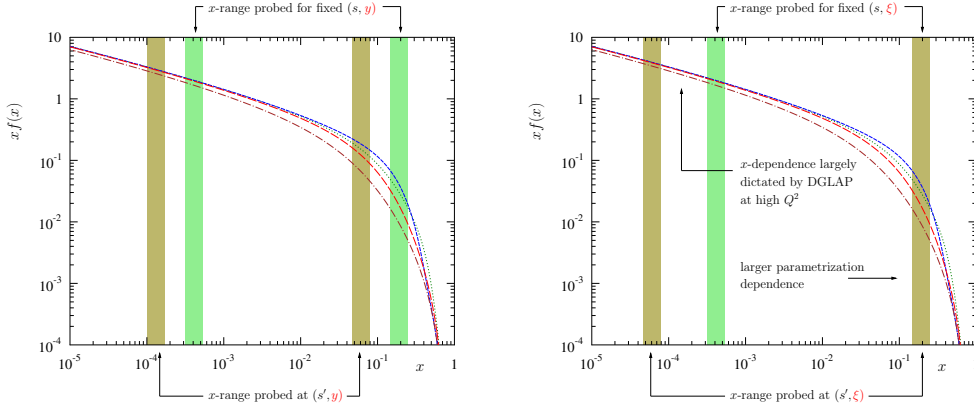


Figure 1: A pictorial representation of the probed x ranges with fixed rapidity y (left) and fixed ξ_1 (right). The curves correspond to the CT10NLO PDFs [2] at $Q^2 = M_W^2$.

where $F^\pm(\xi, H_1, H_2)$ is a function that does not depend explicitly on \sqrt{s} or y . The approximation of Eq. (1.4) should be reasonable if x is small enough, which can be ensured by considering large y . We also note that at large x the power-law approximation would not be a good one and this is the reason why, as in Figure 1, we intend to “align” the x ranges at large- x and not at small x . In the case of W charge asymmetry $\mathcal{A}(\xi_1, \sqrt{s}, H_1, H_2)$, the \sqrt{s} dependence cancels completely,

$$\mathcal{A}(\xi_1, \sqrt{s}, H_1, H_2) = \frac{d\sigma^{\ell^+}/d\xi_1 - d\sigma^{\ell^-}/d\xi_1}{d\sigma^{\ell^+}/d\xi_1 + d\sigma^{\ell^-}/d\xi_1} \approx \frac{F^+(\xi_1, H_1, H_2) - F^-(\xi_1, H_1, H_2)}{F^+(\xi_1, H_1, H_2) + F^-(\xi_1, H_1, H_2)}, \quad (1.6)$$

even if the β was x dependent (as it definitely is). Making a further approximation that the behaviour of small- x PDFs is flavor independent

$$x\bar{q}_i(x, Q^2) \approx xq_i(x, Q^2) \approx N x^{-\beta(Q^2)}, \quad x \ll 1, \quad (1.7)$$

it follows that

$$\mathcal{A}(\xi_1, \sqrt{s}, H_1, H_2) \approx F(\xi_1, H_1), \quad y \gg 0. \quad (1.8)$$

That is, at fixed value of ξ_1 , the W charge asymmetry depends effectively only on the species (proton, nucleus, ...) probed at large x . As a consequence, the prediction is that one should be able to directly compare W charge asymmetry in e.g. p - p and p - Pb collisions at $y^\ell \gg 0$. The same scaling laws can obviously be derived also for $y < 0$ using a scaling variable $\xi_2 \equiv \frac{M_W}{\sqrt{s}} e^{-y}$.

2. Results

In what follows, instead of presenting plots as a function of ξ_1 , we will use the shifted-rapidity variable y_{ref} ,

$$y_{\text{ref}} \equiv y + \log\left(\frac{\sqrt{s_{\text{ref}}}}{\sqrt{s}}\right), \quad (2.1)$$

where $\sqrt{s_{\text{ref}}}$ is a chosen reference c.m. energy. For example, if we take $\sqrt{s_{\text{ref}}} = 7$ TeV, the rapidity variable at $\sqrt{s} = 8$ TeV is shifted by $y \rightarrow y + \log(7\text{TeV}/8\text{TeV}) \approx y - 0.134$. We note that a similar rapidity shift has been recently discussed also in the context of heavy-flavor production [3].

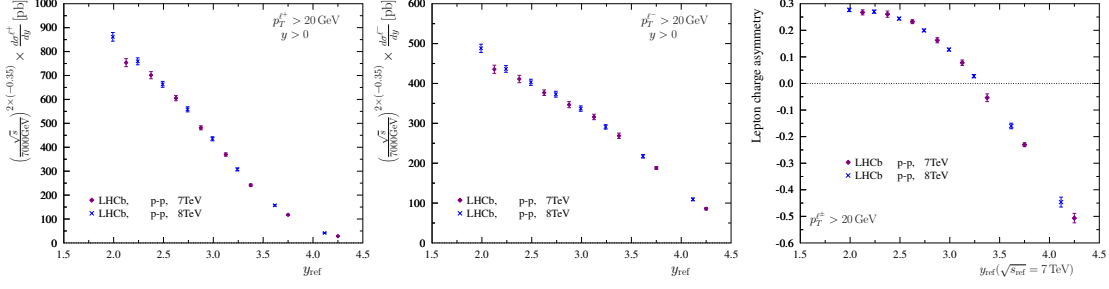


Figure 2: The LHCb data at $\sqrt{s} = 7, 8$ TeV and for W^+ (left), W^- (middle), and charge asymmetry (right).

In Figure 2, we contrast the LHCb $\sqrt{s} = 7$ TeV [4] and $\sqrt{s} = 8$ TeV [5] p-p data against the derived scaling laws. In the case of absolute cross sections we plot the quantity $(\sqrt{s}/7\text{TeV})^{-2\beta} \times d\sigma^{\ell^\pm}(\sqrt{s}, y_{\text{ref}})/dy_{\text{ref}}$, which, as far as Eq. (1.5) is accurate, should be independent of \sqrt{s} . As can be seen from Figure 2 (left and middle panels), the data points indeed line up on a same curve to a very good approximation. The right-most panel of Figure 2 shows the W charge asymmetry as a function of y_{ref} . In agreement with Eq. (1.6), the data points settle roughly on a same curve.

Finally, we test the prediction of Eq. (1.8) against the world data on W charge asymmetry. This is done in Figure 3 where we combine the data from p-p, p-p-bar, p-Pb, and Pb-Pb collisions in a single plot. The prediction is that at fixed value of y_{ref} ,

$$\begin{aligned} y \gg 0 : \mathcal{A}(p\bar{p}) &\approx \mathcal{A}(pp) \approx \mathcal{A}(p\text{Pb}) \quad (\text{probe p at large } x) \\ y \ll 0 : \mathcal{A}(p\text{Pb}) &\approx \mathcal{A}(\text{PbPb}) \quad (\text{probe Pb at large } x) \end{aligned}$$

To keep the plot readable, the p-p and p-p-bar data are plotted only for $y > 0$ and Pb-Pb data only $y < 0$. Indeed, to a good approximation, the data align on curve which corresponds to the charge asymmetry in p-Pb collisions. In the case of Tevatron p-p-bar data one has to go to rather large y_{ref} to see the unification with the LHCb data as the \sqrt{s} is lower and probed x values too large for the approximation made in Eq. (1.4) and Eq. (1.7) to be accurate.

Having now seen that the derived scaling laws are indeed rather good estimations, we can turn them into a tool for precision physics. To this end, we consider the double ratio $\mathcal{D}_{8/7} = (R_{8/7}^+)/ (R_{8/7}^-)$, where

$$R_{8/7}^+ = \frac{d\sigma^{W^+}(\sqrt{s} = 8\text{TeV})}{d\sigma^{W^+}(\sqrt{s} = 7\text{TeV})}, \quad R_{8/7}^- = \frac{d\sigma^{W^-}(\sqrt{s} = 8\text{TeV})}{d\sigma^{W^-}(\sqrt{s} = 7\text{TeV})}. \quad (2.2)$$

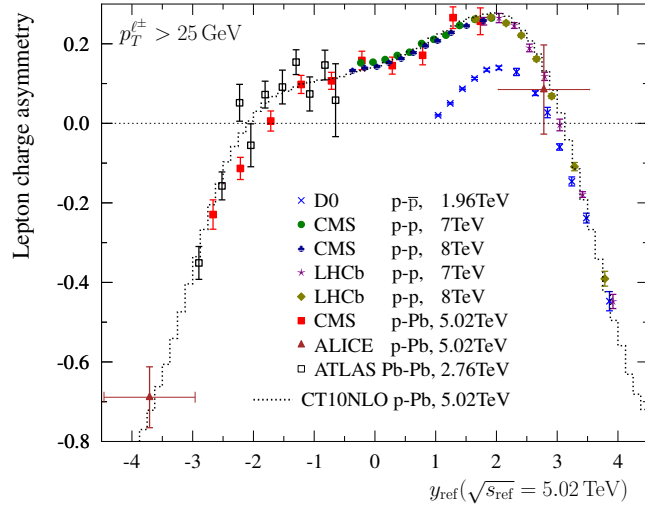


Figure 3: The world data on charge asymmetry as a function of y_{ref} .

In Figure 4, we show the predictions as obtained by using PDF4LHC15_30 set [6] of PDFs. As can be seen, the PDF uncertainty becomes clearly narrower when the ratio is formed at fixed y_{ref} than when the ratio is taken at fixed y . The smaller uncertainties follow from a better cancellation of the large- x PDF uncertainties as now at fixed y_{ref} the probed large- x regions are the same for both c.m. energies (see Figure 1). This observation should e.g. help in understanding the deviations from the NLO predictions for the integrated double ratio recently observed by the LHCb [5].

3. Summary

We have reported on a study of scaling properties of inclusive W^\pm production. The approximate scaling laws we have derived facilitate an easy understanding of the \sqrt{s} dependence of the absolute cross sections and charge asymmetry. We have also demonstrated how one can directly compare measurements in different collision systems. As a by product, we have found that when the ratios of W^\pm cross sections between different \sqrt{s} are taken at fixed value of the scaling variable $\xi_1 = \frac{M_W}{\sqrt{s}} e^y$, the predictions are particularly robust against PDF errors and will facilitate tests of the Standard Model with reduced PDF uncertainty.

Acknowledgments

The work of ÉC has been supported by the European Research Council, under the ‘‘QuarkGluon-PlasmaCMS’’ #259612 grant. H.P. acknowledges the funding from Academy of Finland, Project 297058; the European Research Council grant HotLHC ERC-2011-StG-279579 ; Ministerio de Ciencia e Innovaci3n of Spain and FEDER, project FPA2014-58293-C2-1-P; Xunta de Galicia (Conselleria de Educaci3n) - H.P. is part of the Strategic Unit AGRUP2015/11.

References

- [1] F. Arleo, É. Chapon and H. Paukkunen, Eur. Phys. J. C **76** (2016) no.4, 214 doi:10.1140/epjc/s10052-016-4049-1 [arXiv:1509.03993 [hep-ph]].
- [2] H. L. Lai, M. Guzzi, J. Huston, Z. Li, P. M. Nadolsky, J. Pumplin and C.-P. Yuan, Phys. Rev. D **82** (2010) 074024 doi:10.1103/PhysRevD.82.074024 [arXiv:1007.2241 [hep-ph]].
- [3] R. Gauld, JHEP **1705** (2017) 084 doi:10.1007/JHEP05(2017)084 [arXiv:1703.03636 [hep-ph]].
- [4] R. Aaij *et al.* [LHCb Collaboration], JHEP **1412** (2014) 079 doi:10.1007/JHEP12(2014)079 [arXiv:1408.4354 [hep-ex]].
- [5] R. Aaij *et al.* [LHCb Collaboration], JHEP **1601** (2016) 155 doi:10.1007/JHEP01(2016)155 [arXiv:1511.08039 [hep-ex]].
- [6] J. Butterworth *et al.*, J. Phys. G **43** (2016) 023001 doi:10.1088/0954-3899/43/2/023001 [arXiv:1510.03865 [hep-ph]].

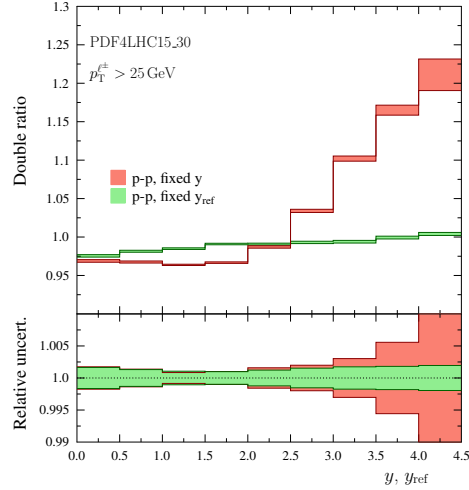


Figure 4: The double ratio $\mathcal{D}_{8/7}$ at fixed rapidity y (red) and at fixed y_{ref} (green). The bands represent the uncertainties from PDF4LHC15_30 PDFs [6].